

Asian Journal of  
**Applied**  
Sciences

## Seismic Design of FRP Reinforced Concrete Structures

<sup>1</sup>M. Kazem Sharbatdar and <sup>2</sup>Murat Saatcioglu

<sup>1</sup>Faculty of Civil Engineering, Semnan University, Semnan, Iran

<sup>2</sup>Department of Civil Engineering, Faculty of Engineering,  
University of Ottawa, Ottawa, Canada

---

**Abstract:** Experimental research has been conducted at the Structures Laboratory of the University of Ottawa to investigate the seismic performance of FRP reinforced concrete structural elements. Large scale columns and beams are being tested under simulated seismic loading. Fiber Reinforced Polymer (FRP) reinforcement is being developed in the form of longitudinal bars and transverse grids for use in new concrete elements in bridges and buildings. Since, this kind of reinforcement shows linear stress-strain characteristics up to failure and has low ductility, serious concerns should be considered about their applicability to earthquake resistant structures. The results of selected tests are summarized in this study, with the assessment of their significance from seismic performance perspective. Column and beam specimens were tested under lateral deformation reversals. The members were reinforced with carbon FRP bars in the longitudinal direction and carbon FRP grids in the transverse direction. Both the columns and the beams sustained a minimum of 2-3% lateral drift ratios, meeting seismic drift limitations of most building codes. Test results indicate that FRP reinforced concrete elements exhibit reduced stiffness and softened response because of the lower elastic modulus of FRP bars. This may suggest reduced spectral values associated with longer vibration periods, as well as increased deformability, resulting in seismic resistant structures for which elastic design approach with sufficient deformability may be appropriate.

**Key words:** Confinement, ductility, earthquakes, FRP bars, reinforced concrete, seismic resistant

---

## INTRODUCTION

Fiber Reinforced Polymer (FRP) reinforcement, in the form of longitudinal and transverse reinforcement, are currently being developed for use in new buildings and bridges (Nanni, 2001). The major driving force behind this development is the superior performance of FRPs in corrosive environments (El-Salakawy *et al.*, 2005). FRP reinforcement has high strength-to-weight ratio, favorable fatigue strength, electro-magnetic transparency and low relaxation characteristics when compared with steel reinforcement, offering a structurally sound alternative in most applications. However, FRP reinforcement shows linear stress-strain characteristics up to failure, without any ductility. The experimental results conducted by Deitz *et al.* (2003) showed that even though some GFRP rebar experienced the ultimate compressive strength approximately 50% of the ultimate tensile strength, the main failure mode was due to low ductility of these bars. This low ductility characteristic of FRP bars poses serious concerns about their applicability to earthquake resistant structures, where seismic energy is expected to be dissipated through inelasticity in members.

---

**Corresponding Author:** Mohammad Kazem Sharbatdar, Semnan University Central Building, Molavi Boulevard, Semnan, Postal Code 35195-363, Iran Tel: 0098-231-3335405 Fax: 0098-231-3335404

Several models were suggested to apply for steel reinforced concrete members such as confined columns for increasing the ductility of those members (Pauly and Priestly, 1991), these models can not directly applied to FRP reinforced members due to non-ductility of this material. FRP bars have different ductility because of different fiber material, new bars were developed to show higher ductility for flexural and shear dominated concrete members (Benmokrane *et al.*, 2002; Tim and Chris, 2003; Toutanji and Saafi, 2000). Experimental test results have shown that a concrete beam reinforced with AFRP bars becomes more flexible in the postcracking range and so a method has been suggested to provide a meaningful quantification of ductility for FRP-reinforced beams (Rashid *et al.*, 2005). The interface behavior of rebars to concrete, bond, was an important issue that were carried and considered in the last decade to show different influential parameters (Maria Antonietta *et al.*, 2007; Focacci *et al.*, 2000; Pecce *et al.*, 2001).

Sharbatdar (2003) developed an analytical model for hysteretic moment-displacement relationship for FRP reinforced columns under constant axial loading. The primary moment-flexural displacement relationship defines the strength boundary and initial stiffness. The main difference of the model, as opposed to the hysteretic models for steel reinforced concrete members, is that the unloading branches of hysteretic loops aim towards the origin of moment-displacement relationship (zero point) due to the elastic behavior of FRP bars in tension. Therefore, inelastic response of FRP reinforced structures can be analyzed by using appropriate models. In order to prevent brittle failure, concrete crushing can be obtained at ultimate prior to the tension failure of FRP provided that the concrete is confined sufficiently and that the section is over-reinforced as opposed to conventional design concept used for steel reinforced sections (Sharbatdar, 2003; Deitz *et al.*, 2003).

Experimental research presented in this study has been underway at the Structures Laboratory of the University of Ottawa to investigate seismic performance of FRP reinforced concrete structural elements. Large scale columns and beams have been tested under simulated seismic loading.

### **Research Significance**

There are uncertainties about the FRP use in new construction; their elongation before the material failure is very small which causes brittle failure. Therefore, codes on FRP reinforced structures, such as Canadian Standards Association CSA 806-02 (2002), Canadian Network of Centres of Excellence on Intelligent Sensing for Innovative Structures (2002) and American Concrete Institute ACI-440 (2001) limited the replacement of steel reinforcement by FRP reinforcement only as flexural reinforcement in beams and shear reinforcements (Nanni, 2001).

Ductility gains importance especially for seismic design of structures. Therefore, investigations on the inelastic behavior of the FRP reinforced sections under cyclic loading are needed in order to understand the overall seismic behavior of the FRP reinforced structures. The inelastic analysis of the structures generally requires complex and difficult calculations. With the advent of computers, several programs have been developed for nonlinear dynamic analysis of steel reinforced concrete structures. However, there is still need for computer programs for the dynamic nonlinear analysis of the FRP reinforced concrete structures.

### **Experimental Program**

The experimental program consists of two types of reinforced concrete elements; (i) square columns and (ii) rectangular beams. They represent portions of column and beam elements between rigidly attached adjoining members and the points of contraflexure, as cantilever specimens. The specimens were reinforced with carbon FRP bars and carbon FRP grids as longitudinal and transverse reinforcement, respectively.

The columns had a 355 mm square cross section with either a 1900 mm height, which resulted in a 2180 mm shear span when measured from the point of application of lateral load, or 1000 mm

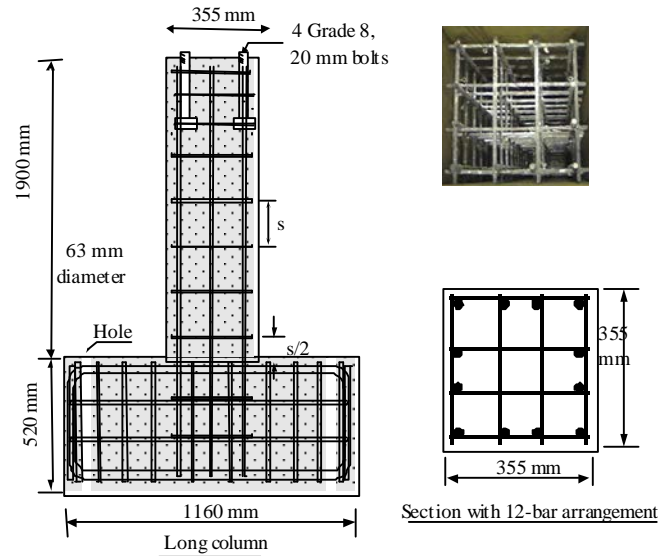


Fig. 1: Details of column specimens

Table 1: Properties of test specimens

Specimen	$f'_c$ (MPa)	Reinforcement arrangement	$\rho$ (%)	S (mm)	L (mm)	P (kN)	P/P0 (%)
<b>Columns</b>							
CFCL3	37	12-9.5 mm bars	0.70	175	1900	1115	27
CFCL4	37	12-9.5 mm bars	0.70	88	1900	1115	27
CFCL8	37	12-9.5 mm bars	0.70	175	1000	1220	30
<b>Beams</b>							
CFB4	40	6-9.5 mm bars (+ve)	0.39	180	1900	0	0
		4-9.5 mm bars (-ve)	0.26				
CFB5	40	6-9.5 mm bars (+ve)	0.39	90	1900	0	0
		4-9.5 mm bars (-ve)	0.26				
CFB2	40	6-9.5 mm bars (+ve)	0.39	90	870	0	0
		4-9.5 mm bars (-ve)	0.26				

height and 1280 mm shear span to increase the imposed shear. This implies that the two longer columns discussed in the study would behave predominantly in the flexure mode and the shorter column would develop significant shear stress reversals. Figure 1 shows the geometric details of specimens. The columns were reinforced with 12-9.5 mm diameter carbon FRP bars, resulting in 0.7% longitudinal reinforcement ratio. The longitudinal bars were extended into the footing by 470 mm. Carbon fibre grids were used as column ties. The grids had nine cells and were manufactured from 6×8 mm rectangular FRP bars with overlapping fibres at intersecting joints. They had a square configuration with an out-to-out dimension of 300 mm. One longitudinal bar was placed in each perimeter corner. The grid spacing was either 88 or 175 mm. Table 1 provides a summary of column properties for the column specimens discussed in this study. The beams had 305 mm width and 405 mm depth. They either had a cantilever length of 1900 mm and a shear span of 1780 mm, or a length of 1000 mm and a shear span of 870. The beams were reinforced asymmetrically to simulate the actual arrangement used in practice. Accordingly, top and bottom reinforcement consisted of 6 and 4-9.5 mm diameter carbon FRP bars, respectively, resulting in 0.39 and 0.26% tension reinforcement ratios in the strong and weak directions, respectively. Carbon fibre grids were used as stirrups. The grids had two cells and were manufactured using 6×8 mm rectangular FRP bars with overlapping fibers at intersecting joints. The perimeter dimensions of grids were 250×350 mm and the resulting total area

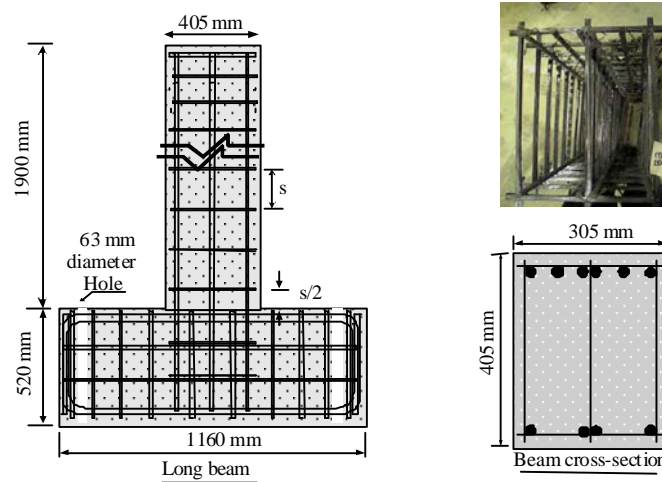


Fig. 2: Details of beam specimens

of transverse reinforcement effective against shear (in the direction of loading) was  $144 \text{ mm}^2$ . The grid spacing was either 90 or 180 mm. Figure 2 and Table 1 provide the details of beam properties.

Two different batches of Normal Portland Cement concrete were used to cast the columns and beams. Separate batches of concrete were used to cast the footings, which were used to secure the specimens to the laboratory strong floor. Concrete strengths during the time of testing were 37 and 40 MPa for the columns and beams, respectively. The longitudinal reinforcement for all specimens was manufactured by Pultrall Inc. with a nominal diameter of 9.5 mm. They were made from high strength carbon fibers and extremely durable vinyl ester resin. The bar surface was sand-coated for improved bond. Sand coating increased the bar diameter to approximately 12 mm. Coupon tests were conducted to establish the stress-strain relationship in tension. The relationship indicates linear behavior with an average tensile strength of 1450 MPa and a modulus of elasticity of 122,000 MPa. The stress-strain relationship of FRP bars in compression was difficult to establish by tests because of the possibility of encountering stability failure. Therefore, short samples, having lengths equal to 2-5 times the bar diameter were tested under direct compression until failure. The average modulus of elasticity in compression was found to be 23,000 MPa, which was approximately 20% of the value in tension. The failure stress in compression varied between 240 and 310 MPa. These values correspond to 16-21% of tensile strength. The failure strain in compression varied between 1 and 1.3%. The failure in direct compression was caused either by delamination of fibers and crushing of resin or by splitting of bars longitudinally. The NEFMAC grids used as transverse reinforcement were manufactured by forming flat grids through a pin-winding process, similar to filament winding. The product used in the current phase of experimental research was reported to have a specific gravity of  $1.4 \text{ t m}^{-3}$  and a modulus of elasticity of 100,000 MPa, by the manufacturer. The grids used as column ties had a square configuration. These grids were manufactured using cross FRP bars, each having a  $6 \times 8 \text{ mm}$  rectangular cross-section, forming nine equal-size square openings. The grids used as beam stirrups had two rectangular cells, simulating a perimeter hoop with a crosstie. The stress-strain relationships, established through coupon tests under direct tension indicate a maximum tensile strength of 1230 MPa and an elastic modulus of 76,335 MPa. These grids are known to have weak joints against maintaining the stability of compression bars against buckling, there was no such failure observed during the column tested reported in this study. The test setup consisted of a horizontal actuator to apply the lateral load, supported by two steel A-frames and two vertical actuators for the application of axial

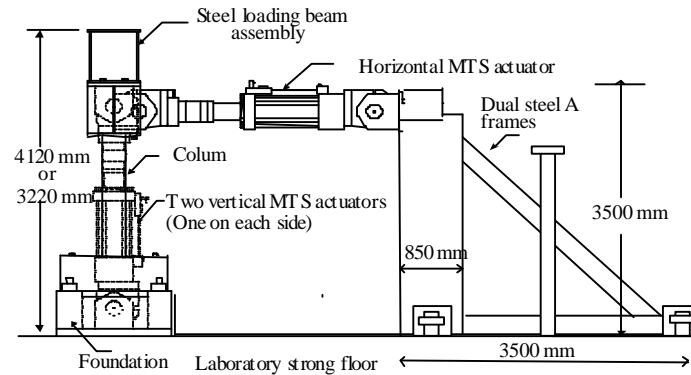


Fig. 3: Test setup

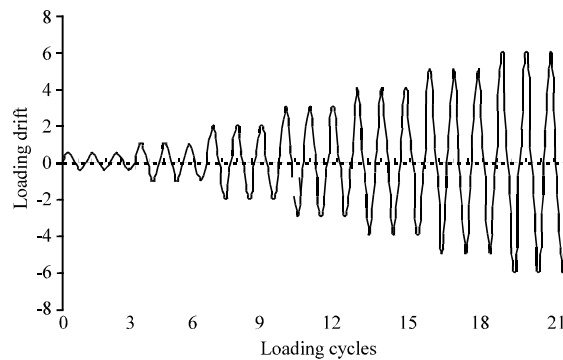
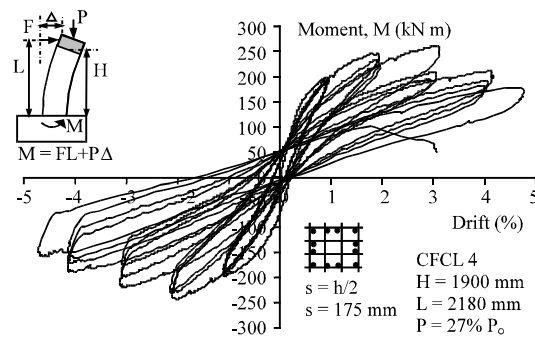


Fig. 4: The deformation history for lateral loading

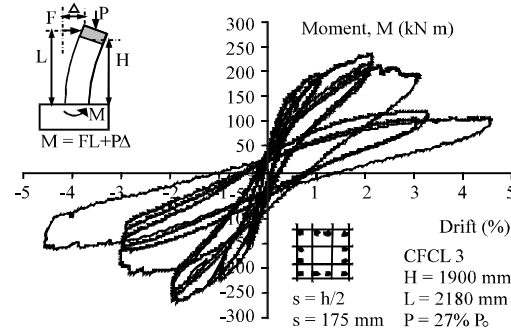
compression on the columns. Figure 3 shows the test setup. The same setup was used for both the columns and beams. Therefore, the beams were tested vertically. The axial load was applied first and was maintained at a constant level through the test. The horizontal load was applied in the deformation control mode. Lateral deformation reversals were applied with three cycles at each of the incrementally increasing drift level. The loading program followed is shown in Fig. 4.

### Test Results

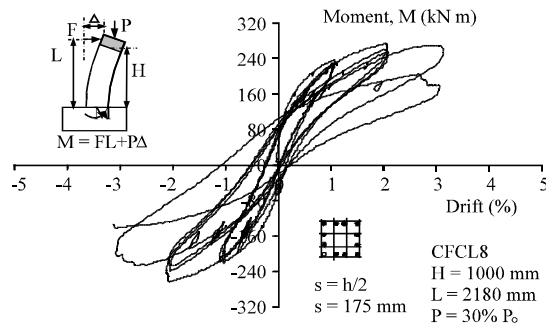
Force-deformation hysteretic characteristics of columns and beams, showing their strengths and deformability, are expressed in term of hysteretic relationships. Figure 5 and 6 show experimentally recorded hysteretic moment-drift relationships for all the specimens. Figure 4 indicates that columns CFCL3 and CFCL4 both developed a 2% lateral drift ratio with little strength degradation. Both columns showed flexure dominant response. Column CFCL4, with closely spaced grids and approximately 62% of the confinement reinforcement required by CSA S806-02, showed increased deformability, with lateral drift ratios reaching up to 3 at 20% strength decay in the direction of first load excursion and 25% decay in the opposite direction. The column was able to sustain 4% lateral drift after 30 and 37% strength decay in the two directions, respectively. The column failed during the second cycle at 5% lateral drift when the compression bars showed local fibre buckling leading to bar failure in compression. Maximum strains recorded in longitudinal bars were 0.93 and 0.55% in tension and compression, respectively. The grids developed 0.5% strain in tension, a value higher than the conservative limit of 0.4% assumed in CSA S806-021 for design. Column CFCL3, with a wider grid spacing of 175 mm and about 31% of the confinement reinforcement required by CSA S806-021 showed brittle behavior shortly after 2% lateral drift, experiencing about a 50% drop in moment



(a) Column CFCL4



(b) Column CFCL3



(c) Column CFCL8

Fig. 5: Experimentally recorded column moment-lateral drift hysteretic relationships

resistance at the end of 3% drift cycles. The maximum strains recorded in longitudinal bars were 0.76 and 0.50% in tension and compression, respectively. The confinement mechanism could not be fully activated in this column because of the wide spacing of grids. The recorded tensile strain in the grids was limited to 0.31%. Column CFCL8 was companion to column CFCL3, except for its shorter length of 1000 mm. This resulted in a shear span of 1280 mm and associated increase in shear force reversals. The column was confined with 9-cell CFRP grids. This resulted in 192 mm<sup>2</sup> of transverse reinforcement in each cross-sectional direction. This amount was equal to 43% of the amount required by CSA S806-02<sup>2</sup> for concrete confinement. The grid spacing was 175 mm, which was approximately twice the maximum spacing permitted by CSA S806-02. The column was subjected to a constant compressive force of 30% of its concentric capacity. The hysteretic relationship shown in Fig. 5

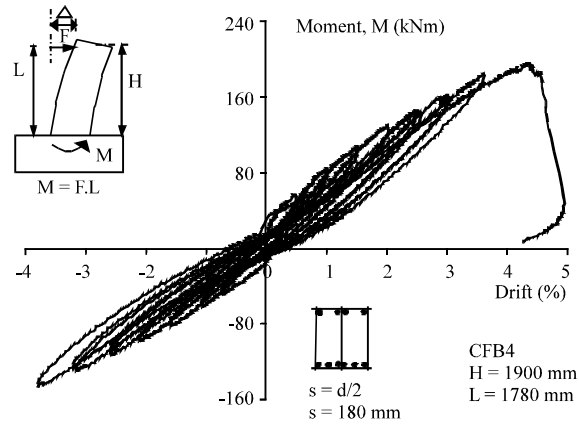
indicates that the column showed stable hysteresis loops up to 2% drift ratio, but developed severe strength decay during the second cycle at 3% drift. The column failed during pulling at the second cycle of 3% drift due to the instability of FRP bars in compression and crushing of concrete. The transverse reinforcement provided was sufficient to prevent shear (diagonal tension) failure, though the column showed increased diagonal cracking as compared to the companion column with a longer height (CFCL3). Strain gauge readings indicated that the FRP bars experienced a maximum of 0.84 and 0.63% strains in tension and compression at the end of test, respectively. The FRP grids experienced a maximum of 0.56% tensile strain, which is 80% higher, due to the increased shear applied on the column, than that recorded in column CFCL3.

The beam hysteretic relationships are shown in Fig. 6. Beams CFB4 and CFB5 were companion specimens with approximately 1.8 m shear span, except for the grid spacing. CFB4 had 180 mm grid spacing, corresponding to  $d/2$  and CFB5 had 90 mm grid spacing, corresponding to  $d/4$ . Both beams were designed to experience tensile rupturing of FRP bars at or shortly after the onset of concrete crushing. The hysteretic relationships indicate essentially elastic response, with gradual degradation of effective elastic stiffness due to progressive cracking under reversed cyclic loading. While both beams experienced 3% drift in the strong direction, the drift capacity was limited to 3 and 2% for CFB4 and CFB5, respectively, in the weak direction. The beams experienced softer response, as compared to the columns discussed earlier, because of the absence of accompanying axial compression. CFB4 experienced significant diagonal cracking on the side faces, in addition to progressively increasing flexural cracking. However, the diagonal cracking was controlled more effectively in CFB5 due to the reduced spacing of transverse grid reinforcement. This also resulted in controlled softening of CFB5 in the strong direction, with 185 kN m of moment resistance at 3% drift, as compared to 156 kN m moment resistance in CFB4 at the same levels of lateral drift. The strain readings indicated 0.0125 and 0.0120 tensile strains in the longitudinal reinforcement of CFB4 and CFB5, respectively, before rupturing in tension at about 4% lateral drift. The maximum compressive strain readings in FRP longitudinal bars were limited to 0.0038 and 0.0028 in CFB4 and CFB5, respectively. The transverse grid reinforcement developed maximum tensile strains of 0.0044 to 0.0040. Beam CFB2 had reduced shear span and increased shear stress reversals. However, the beam was reinforced for shear with closely spaced grid reinforcement, resulting in 55% higher area of shear reinforcement than that recommended by CSA S806-021. The reduction in grid spacing increased the effectiveness of shear resistance while enhancing concrete confinement. Hence, the beam was able to develop its flexural capacity without a premature shear failure. The hysteresis loops showed near elastic behaviour with some stiffness degradation due to concrete cracking, up to 3% drift ratio. Degradation of strength began at the first cycle of 3% drift and continued until 4% drift ratio. At this level of deformation, all the 4 positive moment bars ruptured in tension causing the beam to lose its flexural resistance in the weak direction. The beam was able to resist severely reduced loading in the strong direction when pushed to 5% drift before rupturing all the negative bars.

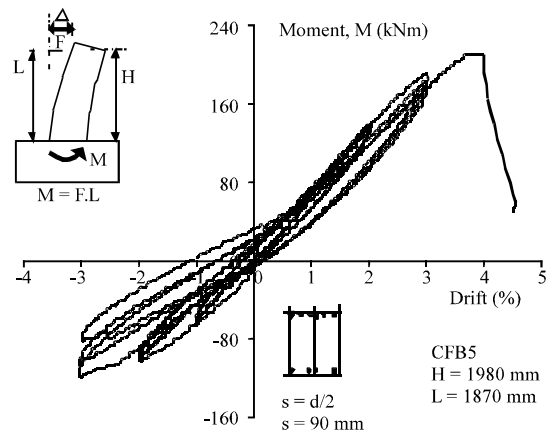
### **Design Implications**

Flexural capacities of FRP reinforced concrete beams were computed using the plane section analysis commonly employed for steel reinforced concrete members in flexure. The analysis was conducted to establish moment-curvature relationships. Experimentally recorded moment-curvature relationships were also obtained for comparison. The experimental relationships were computed from strain gauge data recorded at the beam critical section, as well as LVDT readings within the critical beam region, giving average strains over a gauge length of 300 mm. The curvatures obtained from LVDT readings provided slightly lower values than those obtained by strain gauges, because they represented average curvatures over the gauge length, rather than the maximums recorded at the critical section. Comparisons of moment-curvature relationships, shown in Fig. 7, indicate that the design

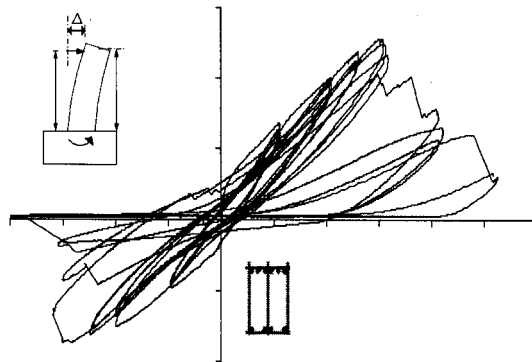




(a) Beam CFB4



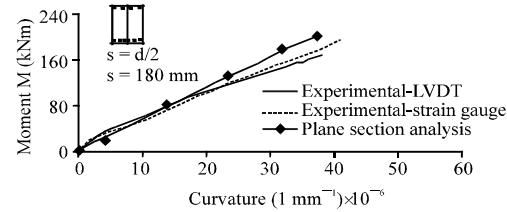
(b) Beam CFB5



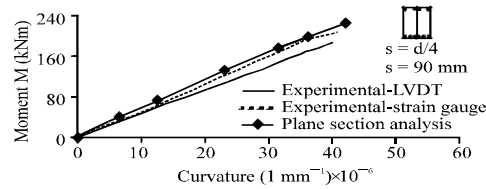
(c) Beam CFB2

Fig. 6: Experimentally recorded beam moment-lateral drift hysteretic relationships

approach employed for conventional steel reinforced concrete beams can be used for the design of FRP reinforced concrete beams, as recommended by CSA S806-02 (2002).

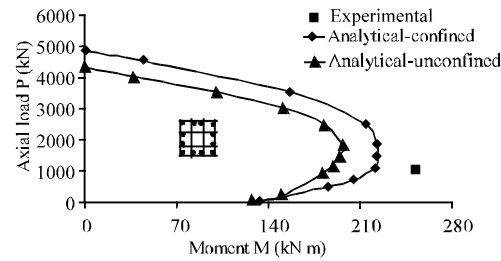


(a) Beam CFB4

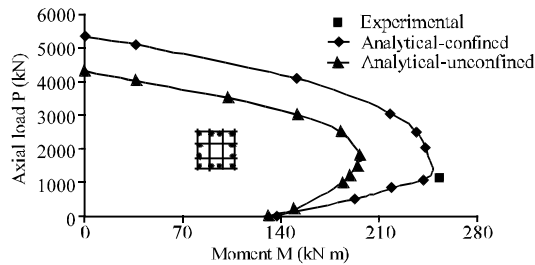


(b) Beam CFB5

Fig. 7: Moment-curvature relationships for FRP reinforced concrete beams



(a) Column CFCL3



(b) Column CFCL4

Fig. 8: Axial force-moment interaction diagrams for FRP reinforced concrete column

The applicability of the plane-section analysis to FRP reinforced column design was also verified. Column axial force-moment interaction diagrams were constructed twice, first using unconfined concrete and secondly the confined concrete model the results plotted in Fig. 8 include experimentally obtained column capacities for two of the columns. The figure clearly shows the applicability of conventional plane section analysis to the computation of axial force-moment interaction diagrams for FRP reinforced concrete elements.

Two design approaches may be used to design FRP reinforced concrete elements. One is to allow sufficiently high safety margin in design against tensile rupturing of bars and ensuring elastic behaviour during service loads and accepting brittle failure under ultimate load conditions initiated either by FRP rupturing in tension or concrete crushing in compression. The other approach is to reduce the safety margin while maintaining elastic behaviour under service loads and over-reinforcing members with FRP reinforcement to prevent bar rupturing at ultimate and promoting ductile failure of compression concrete at ultimate with appropriate concrete confinement. Three different flexural modes of failure were observed in the specimens tested; (i) crushing of concrete due to compression failure of concrete (ii) stability failure of FRP bars in compression and (iii) rupturing of tension reinforcement. The failure of columns under high axial compression and reversed cyclic loading was initiated by the crushing of cover concrete, followed by the buckling of FRP bars in compression and subsequent crushing of core concrete. Tension rupturing of FRP reinforcement occurred in beams, which were not over-reinforced. The type of tension failure was very similar to that observed in coupon tests, where the failure took place within approximately 150 mm segment of the bar, with fibers rupturing randomly at different locations, displaying clear delamination of ruptured fibers from the resin.

While both design philosophies; (i) allowing bar rupturing at ultimate but providing increased safety margin in design and (ii) over-reinforcing members while confining their compression concrete to promote concrete crushing at ultimate prior to bar rupturing, may be defended for design under gravity and wind loading. During a strong earthquake, however, because of the uncertainties associated with seismic design loads, it may be prudent not to allow bar rupturing under any condition. This implies that the members should be confined with properly designed transverse reinforcement in all critical regions. An important aspect of earthquake resistant design is the dissipation of seismic induced energy through significant yielding. This is not possible in FRP reinforced concrete, though some dissipation of energy can be achieved through concrete confinement, as it is also done in steel reinforced concrete columns subjected to high axial compression, above the balanced load level. On the other hand, FRP reinforced concrete exhibits a softer response within the effective elastic range, with extensive cracking of concrete, because of low elastic modulus of FRP reinforcement. This results in increased deformability, with elastic deformations approaching to similar levels as those attained in steel reinforced concrete elements beyond yielding. It also results in longer vibration periods in buildings, with potentially reduced seismic force demands. Figure 9 shows a design response spectrum and the estimates of a typical low-rise concrete building with steel and FRP reinforcement, qualitatively. As demonstrated, elastic seismic force demands in FRP reinforced concrete structures may be substantially lower, depending on the characteristics of the design response spectrum and the dynamic characteristics of buildings.

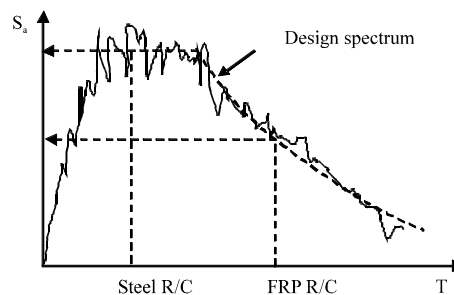


Fig. 9: Effect of the lengthening of period on design force levels

## CONCLUSION

The several conclusions can be drawn from the research presented in this study. FRP reinforced concrete structural elements can be designed for flexure, using the plane section analysis employed for steel reinforced concrete elements, to sustain the required levels of seismic forces.

Tests of large-scale structural components under reversed cyclic loading indicate that FRP reinforced concrete beams can attain a lateral drift ratio of up to 3%, while essentially remaining elastic, though softened due to cracking. FRP reinforced concrete columns under approximately 30% of their concentric capacity can develop 2-3% lateral drift ratios, depending on the level of concrete confinement. The deformability of these elements is sufficiently high to suggest that they can be employed in seismically active regions.

Earthquake resistant design of FRP reinforced concrete structures may be based on elastic member behaviour while taking advantage of relative flexibility of FRP material and also FRP reinforced concrete and associated elongations in the fundamental period of structures, attracting lower spectral accelerations.

More experimental tests including large scale external beam-column concrete joints reinforced with FRP grids and rebars have been conducted at the same lab to investigate the seismic behaviour of joints at this kind of new concrete structures and also generate more data in this regard.

## ACKNOWLEDGMENT

The research reported in this study was made possible by the financial supports from the University of Ottawa. The authors would like to express their gratitude to organization and staffs for their financial and technical supports.

## REFERENCES

- Benmokrane, B., P. Wang, T.M. Ton-That, H. Rahman and J.F. Robert, 2002. Durability of glass fiber-reinforced polymer reinforcing bars in concrete environment. *J. Compos. Constr. ASCE*, 6: 143-153.
- Deitz, D.H., I.E. Harik and H. Gesund, 2003. Physical properties of glass fiber reinforced polymer rebars in compression. *J. Compos. Constr. ASCE*, 7: 363-366.
- El-Salakawy, E., B. Brahim, A. El-Ragaby and N. Dominique, 2005. Field investigation on the first bridge deck slab reinforced with glass FRP bars constructed in Canada. *J. Compos. Constr. ASCE*, 9: 470-479.
- Focacci, F., A. Nanni and C.E. Bakis, 2000. Local bond-slip relationship for FRP reinforcement in concrete. *J. Compos. Constr. ASCE*, 4: 24-31.
- Maria Antonietta, A., L. Marianovella and P. Marisa, 2007. Bond performances of FRP Rebars-Reinforced concrete. *J. Mater. Civil Eng. ASCE*, 19: 205-213.
- Nanni, A., 2001. North America design guidelines for concrete reinforcement and strengthening using FRP: Principles, applications and unresolved issues. *Proceeding of the FRP Composites in Civil Engineering Conference*, Dec. 12-15, Hong Kong, pp: 61-72.
- Pauly, T. and M.J.N. Priestly, 1991. *Seismic Design of Reinforced Concrete and Masonry Buildings*. John Wiley and Sons, New York.
- Pecce, M., G. Manfredi, R. Realfonzo and E. Cosenza, 2001. Experimental and analytical evaluation of bond properties of GFRP bars. *J. Mater. Civil Eng. ASCE*, 13: 282-290.
- Rashid, M.A., M.A. Mansur and P. Paramasivam, 2005. Behavior of Aramid Fiber-reinforced polymer reinforced high strength concrete beams under bending. *J. Compos. Constr. ASCE*, 9: 117-127.

- Sharbatdar, M. Kazem, 2003. Concrete columns and beams reinforced with FRP Bars and grids under monotonic and reversed cyclic loading. Ph.D. Thesis, University of Ottawa.
- Tim, S. and B. Chris, 2003. Shear Analysis of concrete with brittle reinforcement. J. Compos. Constr. ASCE, 7: 323-330.
- Toutanji, H.A. and M. Saafi, 2000. Flexural behavior of concrete beams reinforced with glass fiber-reinforced polymer, GFRP bars. ACI Structural J., 97: 712-719.